ACS APPLIED MATERIALS & INTERFACES

Surfaces, Interfaces, and Applications

Diphylleia Grayi Inspired Stretchable Hydrochromics with Large Optical Modulation in Visible-Near Infrared Region

Guofa Cai, Jiangxin Wang, Alice Lee-Sie Eh, Jingwei Chen, kai qian, Jiaqing Xiong, Gurunathan Thangavel, and Pooi-See Lee

ACS Appl. Mater. Interfaces, **Just Accepted Manuscript** • DOI: 10.1021/acsami.8b12490 • Publication Date (Web): 01 Oct 2018

Diphylleia Grayi Inspired Stretchable Hydrochromics with Large Optical Modulation in Visible-Near Infrared Region

Guofa Cai, Jiangxin Wang, Alice Lee-Sie Eh, Jingwei Chen, Kai Qian, Jiaqing Xiong, Gurunathan Thangavel, and Pooi See Lee*

Author Address: *School of Materials Science and Engineering, Nanyang Technological University, 639798, Singapore*

ABSTRACT

Some animals and plants in nature are endowed with elegant color-changing ability, which inspired the developments of biomimetic systems with multifunctionality, such as controllable colors, transmittance, and mechanical pliability that are significant for the development of energy-efficient and deformable chromic devices, such as wearable displays, smart windows, decorative architectures, camouflage devices, *etc*. Inspired by the color-changing ability of *diphylleia grayi* (commonly known as skeleton flower), we developed a porous PDMS film that dynamically and dramatically changes its color by the adsorption/desorption of minute amount of water (5 g m^{-2}) or other solvents. This hydrochromic phenomenon was analyzed in detail and it matched well with the Mie scattering theory. The porous PDMS film of about 0.4 mm thick exhibits a large optical modulation (about 75~80%) in the broad visible and near infrared region and coloration speed of less than 9 mins. Additionally, the PDMS film can sustain uniaxial strain up to 100% at both transparent and colored states. We believe this new strategy to develop highly scalable porous PDMS film offers a practical route to realize bionic and botanic inspired deformable energy-efficient façade, chromogenic wearables, smart window, smart display, and camouflage *etc*.

KEYWORDS: Stretchable hydrochromic device; Porous poly(dimethylsiloxane) film; Bionics; Smart window; Mie scattering

Smart color-changing phenomena are widespread in nature ranging from animals to plants, mimicking this function is of great significance in scientific and engineering fields. Organisms utilized their color-changing ability for disguising, mating, warning, communicating or displaying etc.[1-4] Pigmentary color and structural color are the two main color-changing ways that exist in the biological world, which are generated through absorbing and reflecting visible light by changing geometries and refractive index, respectively.[5] Color changing mechanism of organisms is due to the modifications in pigments, geometries, or their combinations. For instance, *cephalopods* (cuttlefish, octopuses, squid) and *chameleons* can rapidly alter their skin colors through the absorption and reflection of visible light through the chromatophore pigment cells and iridocytes cells.[6,7] Inspired by the color-shifting ability of these animals, scientists and engineers have developed pioneering materials and systems to mimic such functions. Rogers and colleagues reported an adaptive optoelectronic camouflage system combined by multiplexed arrays of actuators and photodetectors on flexible substrate, which are capable of producing black-and-white patterns to match the surroundings.[8] Bao and colleagues reported a stretchable electronic skin which comprised of a pressure sensor and a stretchable electrochromic device, the e-skin colour can be controlled by changing the applied pressure.[9] Zhao and coworkers designed a soft electro-mechano-chemical system that exhibited various kinds of fluorescent geometries under the control of electric fields.[10] Shepherd and coworkers recently furthered these advancements by illustrating a user interactive e-skin, which exhibits dynamic coloration and sensory feedback from internal and external stimuli.[11] Despite these achievements, all the aforementioned devices still require electric field to maintain or change their light/colour, which are not ideal for the establishment of energy-efficient systems and have some limitations in practical applications (especially in the environments that are lack of electricity). Therefore,

development of a color changing mechanism via natural ways (by ubiquitous stimuli such as force, water and air *etc*) on soft substrates is highly attractive in realizing an actual bionic system. Recently, some research groups used mechanical force to change the optical properties of the polymer thin films with photonic crystals distributed on their surface, such as quasi-amorphous array of silica nanoparticles embedded poly(dimethylsiloxane) (PDMS),[12] nano[13] and micropillar arrays[14] on wrinkled PDMS, shape memory polymers composed of micro-optic components [15] and periodic microhole arrays.[16] However, the modulated wavelength region is narrow (usually in visible range) based on the periodic structure and specific distance between photonic crystals, as governed by the basic principles of the Bragg equation shown in Equation 1:[17-19]

$$\lambda = 2dn_{eff} \quad (1)$$

where λ is the dominant wavelength of reflected light, d is the distance between photonic crystals, and n_{eff} is the effective refractive index of the film. Broad wavelength modulation is very important many aspects. Take smart window for example, the broad wavelength modulation of smart window enables simultaneous controllability of the light and thermal load of the building. Therefore, it is of great interest to expand the modulated wavelength region by natural stimuli.

Indeed, some organisms can alter their skin colors upon varying the amount of water in nature such as beetle's family: *charidotella egregia, tmesisternus isabellae*, *coptocycla, dynastes hercules, cryptoglossa verrucosa and so on*.[5, 20] Take *charidotella egregia* as an example, it exhibits golden coloration in the humidity environment, while a red color was observed in the dry environment.[19] This fascinating color changing phenomenon is enabled by the sophisticated architecture of the cuticle with chirped multilayer structure and a red pigmented layer underneath. A golden color was produced through the multiple reflection and interference of light in the

"chirped" multilayer in which the porous patches are filled with fluid. The filled fluid makes the complex structure into a chirped photonic crystal that provided both specularity and the appropriate spectral selection. The red color is displayed when liquid is expelled from the porous patches which change the multilayer reflector to a translucent slab, leading to an unobstructed view of the underneath red pigmented layer. Besides of animals, plants also display excellent capability in changing their colors upon varying the amount of water. For example, *diphylleia grayi* turns from white color to transparent once in contact with water. It is of great importance to design and fabricate water-activated robust hydrochromic materials, given that water is relatively affordable, safe and ubiquitous. Although there are some attempts in the preparation of water-activated chromic hydrogels based on the periodic structured change of the photonic crystals,[18,21,22] complex experiments process is required to prepare hydrogel photonic crystal bead arrays. Moreover, the unstable hydrogel is not feasible for long-term use without robust sealing. Additionally, hydrogel typically requires scaffold as its structure support. Because of the intrinsic distortion of soft hydrogel, its application as a standalone or discrete device is impeded. Recently, the optical properties of bioinspired or biomimetic PDMS films were studied due to lots advantages of the PDMS such as high optical transmittance, stable, no scaffold required, low cost *etc*.[23, 24]

Inspired by *diphylleia grayi*, we developed a novel, simple, low cost but effective strategy for the design of porous elastomer host based on PDMS that imitates the color-changing behavior of the plant in a broad wavelength range. The porous PDMS as a novel chromic film that exhibits excellent hydrochromic performance including large optical modulation in visible-near infrared region, fast switching speed and high coloration efficiency. Moreover, the color change process is remarkably similar with that of the diphylleia grayi which only depends on the

adsorption/desorption of water. The coloration process of the porous PDMS requires only the adsorption of water, and the bleaching process requires desorption of water in ambient conditions. Finally, its applications on smart glazing and stretchable display are well demonstrated.

RESULTS AND DISCUSSION

The fabrication procedure of the porous PDMS was illustrated in Figure 1a (see Experimental section for details). Firstly, the silicone elastomer base, the curing agent and a certain proportion of LiCl were mixed, and then the PDMS was cured at 120 °C for 3 h. The LiCl will crystallize and form particles during the PDMS curing process. After removing these LiCl particles from the PDMS film by immersing the sample in water, a porous PDMS film (thickness about 0.4 mm) with large size (about 120 cm^2) and high transparency was formed (Figure 1b). Pores with feature sizes ranging from 0.15 to 20 μm are randomly distributed on the surface of the PDMS film, as shown in the field emission scanning electron microscopy (FESEM) image in Figures 1c and d. Moreover, it can been seen from the higher magnification SEM image that the size of most pores ranges from 150 nm to 500 nm (Figure 1d). The depth of the pore ranges from several to decades of micrometer as shown in the cross-section SEM image (Figure S1, Supporting Information). These pores will absorb water once the porous PDMS film is in contact with water due to high capillary force. Meanwhile, the optical properties of the porous PDMS will be drastically changed. The porous PDMS gradually turns to milky white color and lower transmittances were observed when the immersing time is increased (Figure 1e). The porous PDMS film presents a milky white color after immersing in water for 1 hour. This phenomenon closely resembles diphylleia grayi in nature, although the color change process is the reverse.

To quantitatively evaluate the chromic properties and the application of the porous PDMS film on smart glazing, the transmittance of porous PDMS with different thickness and varying ratio of LiCl in the dry state and wet state was monitored as shown in Figure S2 and Figure S3 (Supporting Information), respectively. The transmittance of the porous PDMS films in both dry and wet states decreases with increasing the ratio of LiCl (Figure S2a, Supporting Information). The extent of the reduction in transmittance in the wet state with increasing ratio of LiCl is more drastic than that in dry state. Therefore, the optical modulation ($\Delta T=T_d–T_w$, T_d and T_w is the transmittance in dry and wet states, respectively) increases dramatically with increasing ratio of LiCl up to 1wt% (Figure S2b, Supporting Information). Thereafter, the optical modulation in the near infrared range (800~2250 nm) is continuously increased with increasing ratio of LiCl within 5 wt%, but decreases slightly in the visible range. The optical modulation in both visible and near infrared regions decreases for the porous PDMS film when the ratio of LiCl is over 5 wt%, especially in the visible range. Higher ratio of LiCl will lead to the formation of more pores on the surface of the PDMS, excessive pores will deteriorate the optical properties of the PDMS film due to optical scattering effects. In addition, the transmittance of PDMS film without the presence of LiCl (0 wt% LiCl) in both dry and wet states is almost the same, illustrating that the optical properties of normal PDMS (0 wt% LiCl) is almost unchanged when immersed in water. The optimal ratio of LiCl has been determined to be 5 wt%. The chromic performance of porous PDMS film with different thickness with ratio of 5 wt% LiCl was further investigated (Figure S3, Supporting Information). It can be seen that the optimal thickness of the porous PDMS is around 0.4 mm (Figure S3a, Supporting Information). Although the thin porous PDMS film (of 0.1 mm) presents high transmittance in the dry state, it is also less opaque in the wet state. The thick porous PDMS film (of 0.6 mm) shows low transmittance in the wet state, and remains similar in

the dry state. Therefore, both thin and thick porous PDMS films present small optical modulations as shown in Figure S3b (Supporting Information). The optimum porous PDMS film with thickness of about 0.4 mm and ratio of 5 wt% LiCl exhibits high transmittance in a broad wavelength range (76 ~ 82% in the wavelength range from 500 ~ 2250 nm) in the dry state and low transmittance in the broad wavelength range (around 1% in the wavelength range from 300 ~ 2400 nm) in the wet state (Figure 2a). Moreover, the porous PDMS film shows uniform optical properties even under large scale (about 120 cm^2) at both dry and wet states as shown in Figure 2b and c, respectively. Hence, large optical modulation (about 75~80%) in the broad wavelength range can be attained for the porous PDMS film of 120 cm^2 with thickness of about 0.4 mm and ratio of 5 wt% LiCl in both visible and near infrared region (Figure 2d). The value of the optical modulation is superior than that of most traditional electrochromic,[25-27] photochromic [28-30] and thermochromic materials,[31-33] which can reversibly change their colors by the application of external stimulus, such as electricity, light or heat, respectively. The optical modulation of most of these materials is in the range of from 20% to 60 % in the visible region. The switching speed of the chromic materials from one state to another state is an important factor to determine its potential application. Usually, display devices require a fast response speed. However, relatively slow response speed is acceptable in the smart windows, wearables and camouflage applications. In order to evaluate the switching speed of porous PDMS film, the *in-situ* transmittance vs time spectra in the wetting process and the drying process were analyzed by immersing the sample in water and leaving it in air for drying (Figures 2e and f), respectively. In this work, the switching speed is defined as the time required for the porous PDMS film to reach 90% of its full optical modulation which can be calculated from the *in-situ* transmittance vs time curves. It can be seen that the transmittance drops gradually after immersing porous PDMS film with size of 2×4 cm^2

and thickness of about 0.4 mm in the water (wetting process) and the coloration time takes 518 s (less than 9 mins, Figure 2e). In the reverse process, the transmittance gradually increases to initial state after leaving the porous PDMS film in ambient air condition (25 ^{o}C, 70% humidity) for the drying process and the bleached time takes 3332 s (less than 1 hour, Figure 2f).

In order to understand the chromic mechanism of the porous PDMS film, the wetting and drying processes were investigated in detail. The weight of the film increased upon extending the immersing time of porous PDMS film in water (Figure S4, Supporting Information). Altering the amount of the absorbed water varies the amount of light transmitted (Figure 2e). Only less than 10 wt % of water is required to make the porous PDMS film colored and the coloration time is less than 9 mins. The porous PDMS film changed to the colored states with less than 0.5 mg water per cm^2 (5 g m^{-2}) as shown in Figure 3a, indicating that the porous PDMS film is a water efficient chromic film. When placing the porous PDMS film in the air, the weight of the film decreased and can fully recover to the initial weight (Figure 3a and Figure S4, Supporting Information). Meanwhile the transmittance of the porous PDMS film can be fully recovered (Figure 2f). Additionally, the process is reversible regardless of the amount of water absorbed during the wetting process (Figure S4, Supporting Information). The figure of merit of conventional electrochromic materials is the coloration efficiency (CE), $CE(\lambda)=\Delta OD/\Delta Q=\log(T_b/T_c)/\Delta Q$ (ΔOD and ΔQ denote the change in optical density and unit charge inserted into (or extracted from) the electrochromic film; T_b and T_c the represent the transmittance in the bleached and colored states, respectively).[34] Herein, we define the CE for the porous PDMS film as the change in optical density (ΔOD) per unit weight of water (Δm) absorbed/desorbed into/out from the porous PDMS film in the following Equation 2:

$$CE(\lambda)=\Delta OD/\Delta m=\log(T_d/T_w)/\Delta m \quad (2)$$

where ΔOD and Δm refer to the optical density and the weight of absorbed or desorbed water within per unit area. Therefore, the CE of the wetting and drying process can be calculated from the slope of the linear fit in Figures 3b and c, respectively. It can be seen that the CE for the wetting and drying process are 510 and -587 cm^2 g^{-1}. The large CE value indicates that the porous PDMS film is a water efficient chromic film. In addition, both CE values for the wetting and drying process are almost the same, indicating the excellent reversibility of the porous PDMS film.

To further understand the chromic mechanism of the porous PDMS film, XRD patterns of the porous PDMS and pristine PDMS (0% LiCl) films were studied at the wet state and the dry state (Figure 3d), respectively. It can be seen that the XRD patterns of the normal PDMS (0% LiCl) films have no obvious differences at both wet state and dry state, both patterns have two broad diffraction peaks center at around $2\theta = 5.9°$ and 11.8°, respectively. The broad diffraction peaks can be ascribed to the short-range condensed order of the polysiloxane network. The XRD pattern of the porous PDMS film at the dry state is similar with that of the pristine PDMS, the diffraction peaks only shift slightly towards the higher angle indicating contracted lattice spacing among the short-range ordered polymer chain due to the LiCl crystals. However, the intensity of the diffraction peaks of the same porous PDMS film at the wet state are of low intensity, illustrating that absorbed water causes disorientation in the polysiloxane chains, resulting in more disordered network. The disorderness in the polymer chains upon water absorption in the porous PDMS led to random scattering of light caused by the polymer chains.[35] Therefore, the transmittance is reduced in the porous PDMS film. Additionally, the Mie scattering should be the main reason contributing to the drastic optical properties alterations of the porous PDMS film after immersed in water. Light scattering may be categorized into Rayleigh scattering and Mie

scattering. The spherical coordinate scattering geometry used for Mie scattering corresponding to a single incident light ray on a single spherical particle is shown in Figure 3e (m_o and m in Figure 3e represent the refractive indices of the surrounding medium and the scattering particle, respectively). The scattered radiation intensities are vertically (I_Φ) and horizontally (I_θ) polarized with respect to the scattering plane and can be calculated using this coordinate system as Equations 3 and 4, respectively.[36]

$$I_{\emptyset} = I_0 \frac{\lambda^2}{4\pi^2 r^2} i_1 \sin^2 \emptyset \quad (3)$$

$$I_{\theta} = I_0 \frac{\lambda^2}{4\pi^2 r^2} i_2 \cos^2 \emptyset \quad (4)$$

Where Φ and θ are scattering angles, I_0 and λ represent the intensity and wavelength of the incident light, r is the radius of the spherical particle. The scattering domain is determined by a dimensionless α (Fig.3F), which can be described in the following Equation 5: [37, 38]

$$\alpha = \frac{2\pi r}{\lambda} \quad (5)$$

When $\alpha \geq 0.1$ (particle size≥5 nm), the scattering domain should be Mie scattering (Figure 3f). In this work, the pore size ranges from 0.15 to 20 μm are randomly distributed on the surface of the PDMS film. Therefore, the size of water droplets formed on the surface of the porous PDMS film should be similar with that of the pores when immersing the porous PDMS film into water. The amount of the water droplets increases with increasing the immersing time. As a result, when light passes through the wet porous PDMS film there will be extensive Mie scattering from visible to infrared region (Figure 3g) due to that the wavelength approximately equals to the inhomogeneous size distribution of water droplets from 0.15 to 20 μm,[39-42] leading to the significant drop in the optical transmittance of porous PDMS film when immersed into water. The scattered radiation spectrum within the visible light is consistent with that of the incident

light from the direct sun light, which results in the white color appearance of the porous PDMS film.

Materials and devices with novel features such as being stretchable, flexible and wearable are of significant importance to meet the demanding requirements of multifunctional and complex smart devices.[43-46] Figures 4a and b show the photographs of the porous PDMS film with varying uniaxial strains up to 100% at both dry state and wet state, respectively. During the stretching process, the porous PDMS film maintained the same color in appearance, indicating the excellent water retention under deformation. The transmittance spectra of the porous PDMS film in both dry and wet states were measured over a broad wavelength range from 300 to 2400 nm (Figure 4c). The transmittance of the porous PDMS film increased slightly with increased strain (from 0% to 100% strain) at both dry and wet states (Figure 4c). Therefore, the optical modulation change is indistinguishable with increased strains (Figure 4d), illustrating that our porous PDMS film has superior deformability feature without significantly compromising the chromic properties. The porous PDMS film exhibits excellent chromic properties even under highly deformed state, which is mainly ascribed to the amount of absorbed water that is almost unaffected by the strain state (Figure S5, Supporting Information). It can be seen that the weight of the wet porous PDMS film decreased slightly during the stretching process, only 1.1% weight loss was observed at 100% strain states (the stretching-releasing process is fast in order to reduce the effects of evaporation, each stretching-releasing process less than 5 s). Moreover, the size of the pore or water droplets of porous PDMS film under strain state is still comparable with the wavelength of visible and infrared light (Figure 4e). According to the Mie scattering theory, the porous PDMS film can well maintain its optical property under different strain states in both dry and wet conditions.

In order to illustrate the promising application of porous PDMS film as flexible and energy efficient smart window, a prototype was fabricated by rational design (Figure 5a). The smart window was assembled by employing porous PDMS with size 6×6 cm^2 as chromic layer, the PET casing as water reservoir, VHB tape as spacer and encapsulant. A drain-pipe was installed at the bottom of the smart window which will facilitate the water outflow during the drying process. The spacer thickness is 1 mm, sufficient to fully immerse the porous PDMS film with thickness of about 0.4 mm in the water during the coloration process, while facilitates the rapid evaporation of the absorbed water during the bleaching process. It can be seen that the smart window is transparent before water immersion (Figure 5b). The smart window gradually turns white during the water inflow into the PET casing due to the Mie scattering and becomes fully opaque within half an hour (Figure 5c). The colored smart window can be used to provide privacy for the users, dynamically adjusting solar heat input of the building during the daytime while reducing indoor air-condition energy consumption. When evening rolls around, the water in the reservoir can be released through the drain-pipe, and the absorbed water in the porous PDMS can be evaporated naturally, while the smart window restores to its transparent state. Moreover, the smart window is mechanically robust and can be bended at both bleached and colored states because all components in the device are soft materials (Figures 5d and e) making it very attractive for next-generation deformable energy efficient chromic devices.

The porous PDMS film as display and camouflage applications was also investigated in this work. A porous PDMS with pattern of NTU letters was prepared by molding of normal PDMS as shown in Figure 6. When immersing the transparent PDMS film in water with toluidine blue O (0.5 wt%) as the dye, the purple NTU letters would appeared on the transparent PDMS film (Figure $6a_2$). Toluidine blue O is a thiazine dye and it is cationic in nature. Its chemical structure

is shown in Figure S6a (Supporting Information). The purple color rapidly changed to blue color by simply changing the solvent to ethanol (Figure 6a$_3$, Movie S1, Supporting Information). The color-changed process can be ascribed to the interaction between toluidine blue O and ethanol which would reduce the toluidine blue O (Figure S6b). The purple NTU letters change to blue color with fast switching speed (<1 s) once contact with ethanol, and the sample can change its color back to purple when immersing it into water (Movie S1, Supporting Information). This ability of the soft PDMS film to dynamically switch among multiple modes of coloration is an added advantage for dynamic display application. We believe that the patterned porous PDMS chormic films are versatile for various applications through rational selection of dye and solvent. Furthermore, the color of the patterned porous PDMS films can be recovered to white color (Figure 6a$_4$) and the transparent state (Figure 6a$_5$) by washing and drying the colored films, respectively. Additionally, the as-fabricated display based on porous PDMS is mechanically robust and can be bended, twisted and stretched (Figures 6b, c and d), making it very attractive for stretchable and wearable display applications. In addition, porous PDMS films with shapes of squid and goldfish were also fabricated to illustrate the camouflage applications (Figure S7, Supporting Information). We believe that the simple fabrication coupled with rational design and smart operation of this novel, color-changing porous PDMS film would make these biomimetic systems accessible and useful to different fields.

CONCLUSIONS

In summary, we have developed a novel, low cost and effective strategy for the fabrication of large scale porous PDMS film to imitate the functions of color-changing *diphylleia grayi* in nature, which changed its optical properties in a broad wavelength range by adsorption/desorption of water. The chromic phenomenon was further analyzed in detail and it

matched well with the Mie scattering theory. Most importantly, the porous PDMS film with excellent and reversible chromic performance under stretching can be applied to dynamic smart window or any other dynamic displays and camouflage applications. In the applications such as the camouflage and display, the color of the sample can be rapidly changed (fast switching speed <1 s) by simply changing the solvent. Moreover, the substrate can be easily reused by washing. The new strategy to achieve the inexpensive and highly scalable porous PDMS film may represent a practical route to real-life applications in deformable energy efficient devices such as dynamic high throughput smart window, dynamic display, camouflage, *etc*.

METHODS

Materials. The silicone elastomer base and curing agent (SYLGARD 184) used for preparation of PDMS were purchased from Dow Corning Corporation. Lithium chloride (≥99.0%) and hexane (anhydrous, 95%), and toluidine blue O (technical grade) were purchased from Sigma-Aldrich. Ethanol (absolute for analysis) was purchased from Merck KgaA. Scotch permanent clear mounting tape (VHB 4010) was purchased from 3M Corporation.

Preparation of porous PDMS. The porous PDMS film was fabricated by mixing silicone elastomer base and curing agent with a weight ratio of 10:1. Then, the liquid mixture was diluted with hexane to form a 5 wt% solution. Thereafter, 10 wt% LiCl dissolved in ethanol solution was added into the diluted liquid mixture. Then, the diluted liquid mixture containing dissolved LiCl was transferred onto a watch glass with radius of 6.25 cm. Hexane and ethanol were evaporated by placing the liquid mixture into fume hood for 2 h. The PDMS was cured after degassing and thermal treatment of the diluted liquid mixture at 120 °C for 3 h. Finally, porous PDMS was formed by dissolving the LiCl in water. The PDMS films with different thickness and different amount of LiCl were also prepared.

Fabrication of the smart window. The smart window was assembled by employing porous PDMS as the active chromic layer, a polyethylene terephthalate (PET) casing was used to contain the water, VHB tape as spacer and encapsulant. A drain-pipe was installed at the bottom of the smart window which will facilitate water outflow for the bleaching process.

Characterization: The microstructures, composition and structure of the porous PDMS were characterized using field emission scanning electron microscopy (FESEM, JEOL 7600F) and X-ray diffraction (XRD, Bruker D8). The transmittance spectra of the porous PDMS films were tested by SHIMADZU UV-3600 spectrophotometer. For the strain state transmittance spectra tests, the porous PDMS film was stretched to different strain states and fixed on glass slide.

Supporting Information:

The Supporting Information is available free of charge on the ACS Publications website at DOI: XXXX.

Supporting figures and Mie scattering theory (PDF)

Movie S1 (avi) The hydrochromic processes of the porous PDMS film when contacting with different solvent.

ACKNOWLEDGMENT

This research is supported by the NRF Investigatorship Award NRF-NRFI2015-05 that is supported by the National Research Foundation, Prime Minister's Office, Singapore.

Corresponding Author

*Email Address: pslee@ntu.edu.sg.

REFERENCES AND NOTES

1. Tadepalli, S.; Slocik, J. M.; Gupta, M. K.; Naik, R. R.; Singamaneni, S., Bio-Optics and Bio-Inspired Optical Materials. *Chem. Rev.* **2017,** *117*, 12705-12763.
2. Deravi, L. F.; Magyar, A. P.; Sheehy, S. P.; Bell, G. R. R.; Mäthger, L. M.; Senft, S. L.; Wardill, T. J.; Lane, W. S.; Kuzirian, A. M.; Hanlon, R. T.; Hu, E. L.; Parker, K. K., The Structure–Function Relationships of A Natural Nanoscale Photonic Device in Cuttlefish Chromatophores. *J. R. Soc. Interface* **2014,** *11*, 20130942.
3. Izumi, M.; Sweeney, A. M.; DeMartini, D.; Weaver, J. C.; Powers, M. L.; Tao, A.; Silvas, T. V.; Kramer, R. M.; Crookes-Goodson, W. J.; Mäthger, L. M.; Naik, R. R.; Hanlon, R. T.; Morse, D. E., Changes in Reflectin Protein Phosphorylation are Associated with Dynamic Iridescence in Squid. *J. R. Soc. Interface* **2010,** *7*, 549-560.
4. Braam, J., In Touch: Plant Responses to Mechanical Stimuli. *New Phytologist* **2005,** *165*, 373-389.
5. Liu, F.; Dong, B. Q.; Liu, X. H.; Zheng, Y. M.; Zi, J., Structural Color Change in Longhorn Beetles Tmesisternus Isabellae. *Opt. Express* **2009,** *17*, 16183-16191.
6. Xu, C.; Stiubianu, G. T.; Gorodetsky, A. A., Adaptive Infrared-Reflecting Systems Inspired by Cephalopods. *Science* **2018,** *359*, 1495-1500.
7. Vatankhah-Varnosfaderani, M.; Keith, A. N.; Cong, Y.; Liang, H.; Rosenthal, M.; Sztucki, M.; Clair, C.; Magonov, S.; Ivanov, D. A.; Dobrynin, A. V.; Sheiko, S. S., Chameleon-Like elastomers with Molecularly Encoded Strain-adaptive Stiffening and Coloration. *Science* **2018,** *359*, 1509-1513.
8. Yu, C.; Li, Y.; Zhang, X.; Huang, X.; Malyarchuk, V.; Wang, S.; Shi, Y.; Gao, L.; Su, Y.; Zhang, Y.; Xu, H.; Hanlon, R. T.; Huang, Y.; Rogers, J. A., Adaptive Optoelectronic Camouflage Systems with Designs Inspired by Cephalopod skins. *Proc. Natl Acad. Sci.* **2014,** *111* (36), 12998-13003.
9. Chou, H.-H.; Nguyen, A.; Chortos, A.; To, J. W. F.; Lu, C.; Mei, J.; Kurosawa, T.; Bae, W.-G.; Tok, J. B. H.; Bao, Z., A Chameleon-Inspired Stretchable Electronic Skin with Interactive Colour Changing Controlled by Tactile Sensing. *Nat. Commun.* **2015,** *6*, 8011.
10. Wang, Q.; Gossweiler, G. R.; Craig, S. L.; Zhao, X., Cephalopod-Inspired Design of Electro-mechano-chemically Responsive Elastomers for on-Demand Fluorescent Patterning. *Nat. Commun.* **2014,** *5*, 4899.
11. Larson, C.; Peele, B.; Li, S.; Robinson, S.; Totaro, M.; Beccai, L.; Mazzolai, B.; Shepherd, R., Highly Stretchable Electroluminescent Skin for Optical Signaling and Tactile Sensing. *Science* **2016,** *351*, 1071-1074.
12. Ge, D.; Lee, E.; Yang, L.; Cho, Y.; Li, M.; Gianola, D. S.; Yang, S., A Robust Smart Window: Reversibly Switching from High Transparency to Angle-Independent Structural Color Display. *Adv. Mater.* **2015,** *27*, 2489-2495.
13. Lee, S. G.; Lee, D. Y.; Lim, H. S.; Lee, D. H.; Lee, S.; Cho, K., Switchable Transparency and Wetting of Elastomeric Smart Windows. *Adv. Mater.* **2010,** *22*, 5013-5017.
14. Lee, E.; Zhang, M.; Cho, Y.; Cui, Y.; Van der Spiegel, J.; Engheta, N.; Yang, S., Tilted Pillars on Wrinkled Elastomers as a Reversibly Tunable Optical Window. *Adv. Mater.* **2014,** *26*, 4127-4133.
15. Xu, H.; Yu, C.; Wang, S.; Malyarchuk, V.; Xie, T.; Rogers, J. A., Deformable, Programmable, and Shape-Memorizing Micro-Optics. *Adv. Funct. Mater.* **2013,** *23*, 3299-3306.
16. Li, J.; Shim, J.; Deng, J.; Overvelde, J. T. B.; Zhu, X.; Bertoldi, K.; Yang, S., Switching Periodic Membranes via Pattern Transformation and Shape Memory Effect. *Soft Matter.* **2012,** *8*, 10322-10328.
17. Hiltner, P. A.; Krieger, I. M., Diffraction of Light by Ordered Suspensions. *J. Phys. Chem.* **1969,** *73*, 2386-2389.

18. Tian, E.; Wang, J.; Zheng, Y.; Song, Y.; Jiang, L.; Zhu, D., Colorful Humidity Sensitive Photonic Crystal Hydrogel. *J. Mater. Chem.* **2008,** *18*, 1116-1122.
19. Vigneron, J. P.; Pasteels, J. M.; Windsor, D. M.; Vértesy, Z.; Rassart, M.; Seldrum, T.; Dumont, J.; Deparis, O.; Lousse, V.; Biró, L. P.; Ertz, D.; Welch, V., Switchable Reflector in the Panamanian Tortoise Beetle Charidotella Egregia (Chrysomelidae: Cassidinae). *Phys. Rev. E* **2007,** *76*, 031907.
20. Jolivet, P. H.; Cox, M. L.; Petitpierre, E., Eds, Novel Aspects of the Biology of Chrysomelidae, Springer Netherlands: Dordrecht, **1994**.
21. Du, X.; Wang, J.; Cui, H.; Zhao, Q.; Chen, H.; He, L.; Wang, Y., Breath-Taking Patterns: Discontinuous Hydrophilic Regions for Photonic Crystal Beads Assembly and Patterns Revisualization. *ACS Appl. Mater. Interfaces* **2017,** *9*, 38117-38124.
22. Chen, H.; Yang, F.; Chen, Q.; Zheng, J., A Novel Design of Multi-Mechanoresponsive and Mechanically Strong Hydrogels. *Adv. Mater.* **2017,** *29*, 1606900.
23. Li, K.; Zhang, Y.; Zhen, H.; Wang, H.; Liu, S.; Yan, F.; Zheng, Z., Versatile Biomimetic Haze Films for Efficiency Enhancement of Photovoltaic Devices. *J. Mater. Chem. A* **2017**, *5*, 969-974.
24. Owuor, P. S.; Chaudhary, V.; Woellner, C. F.; Sharma, V.; Ramanujan, R. V.; Stender, A. S.; Soto, M.; Ozden, S.; Barrera, E. V.; Vajtai, R.; Galvão, D. S.; Lou, J.; Tiwary, C. S.; Ajayan, P. M., High Stiffness Polymer Composite with Tunable Transparency. *Mater. Today* **2018**, *21*, 475-482.
25. Cai, G. F.; Wang, J. X.; Lee, P. S., Next-Generation Multifunctional Electrochromic Devices. *Acc. Chem. Res.* **2016,** *49*, 1469-1476.
26. Gu, H.; Guo, C.; Zhang, S.; Bi, L.; Li, T.; Sun, T.; Liu, S., Highly Efficient, Near-Infrared and Visible Light Modulated Electrochromic Devices Based on Polyoxometalates and $W_{18}O_{49}$ Nanowires. *ACS Nano* **2018,** *12*,559–567.
27. Li, R.; Li, K.; Wang, G.; Li, L.; Zhang, Q.; Yan, J.; Chen, Y.; Zhang, Q.; Hou, C.; Li, Y.; Wang, H., Ion-Transport Design for High-Performance Na^+-Based Electrochromics. *ACS Nano* **2018,** *12*, 3759–3768.
28. Wang, W.; Ye, M.; He, L.; Yin, Y., Nanocrystalline TiO_2-Catalyzed Photoreversible Color Switching. *Nano Lett.* **2014,** *14*, 1681-1686.
29. Zhang, H.; Wang, G.; Chen, D.; Lv, X.; Li, J., Tuning Photoelectrochemical Performances of Ag−TiO_2 Nanocomposites via Reduction/Oxidation of Ag. *Chem. Mater.* **2008,** *20*, 6543-6549.
30. Fukuda, K.; Akatsuka, K.; Ebina, Y.; Ma, R.; Takada, K.; Nakai, I.; Sasaki, T., Exfoliated Nanosheet Crystallite of Cesium Tungstate with 2D Pyrochlore Structure: Synthesis, Characterization, and Photochromic Properties. *ACS Nano* **2008,** *2*, 1689-1695.
31. Wang, S.; Liu, M.; Kong, L.; Long, Y.; Jiang, X.; Yu, A., Recent Progress in VO_2 Smart Coatings: Strategies to Improve the Thermochromic Properties. *Prog. Mater Sci.* **2016,** *81*, 1-54.
32. Warwick, M. E. A.; Binions, R., Advances in Thermochromic Vanadium Dioxide Films. *J. Mater. Chem. A* **2014,** *2*, 3275-3292.
33. Ke, Y.; Zhou, C.; Zhou, Y.; Wang, S.; Chan, S. H.; Long, Y., Emerging Thermal-Responsive Materials and Integrated Techniques Targeting the Energy-Efficient Smart Window Application. *Adv. Funct. Mater.* **2018,** 1800113.
34. Cai, G. F.; Darmawan, P.; Cheng, X.; Lee, P. S., Inkjet Printed Large Area Multifunctional Smart Windows. *Adv. Energy Mater.* **2017,** *7*, 1602598.
35. Rybin, M. V.; Khanikaev, A. B.; Inoue, M.; Samusev, K. B.; Steel, M. J.; Yushin, G.; Limonov, M. F., Fano Resonance between Mie and Bragg Scattering in Photonic Crystals. *Phys. Rev. Lett.* **2009,** *103*, 023901.

36. Hahn David W., Light Scattering Theory. University of Florida, **2009**. (Retrieved 2017-09-22).
37. Träger F., Springer Handbook of Lasers and Optics. Springer Science & Business Media, 2012.
38. Bohren, C. F.; Huffmann, D. R. Absorption and Scattering of Light by Small Particles. Wiley-VCH Verlag GmbH & Co. KGaA, New York, **2010**.
39. van de Hulst H. C., Light Scattering by Small Particles. Wiley-VCH Verlag GmbH & Co. KGaA, New York, **1957**. (Paperback by Dover Publications, New York, 1981).
40. Bhattacharjee, S., DLS and Zeta Potential – What They are and What They are not? *J. Controlled Release* **2016,** *235*, 337-351.
41. Z. Ghassemlooy, W.O. Popoola, Terrestrial Free-space Optical Communications, in: S. Ait Fares, F. Adachi (Eds.), Mobile and Wireless Communications Network Layer and Circuit Level Design, IN TECH, Rijeka, **2010,** 355–392
42. Li, Q.; Zhang, Y.; Shi, L.; Qiu, H.; Zhang, S.; Qi, N.; Hu, J.; Yuan, W.; Zhang, X.; Zhang, K.-Q., Additive Mixing and Conformal Coating of Noniridescent Structural Colors with Robust Mechanical Properties Fabricated by Atomization Deposition. *ACS Nano* **2018,** *12*, 3095-3102.
43. Rogers, J. A.; Someya, T.; Huang, Y., Materials and Mechanics for Stretchable Electronics. *Science* **2010,** *327*, 1603-1607.
44. Wang, C.; Hwang, D.; Yu, Z.; Takei, K.; Park, J.; Chen, T.; Ma, B.; Javey, A., User-interactive Electronic Skin for Instantaneous Pressure Visualization. *Nat. Mater.* **2013,** *12*, 899-904.
45. Cai, G. F.; Wang, J. X.; Lin, M.-F.; Chen, J. W.; Cui, M. Q.; Qian, K.; Li, S. H.; Cui, P.; Lee, P. S., A Semitransparent Snake-like Tactile and Olfactory Bionic Sensor with Reversibly Stretchable Properties. *NPG Asia Mater.* **2017,** *9*, e437.
46. Someya, T.; Bao, Z.; Malliaras, G. G., The Rise of Plastic Bioelectronics. *Nature* **2016,** *540*, 379.

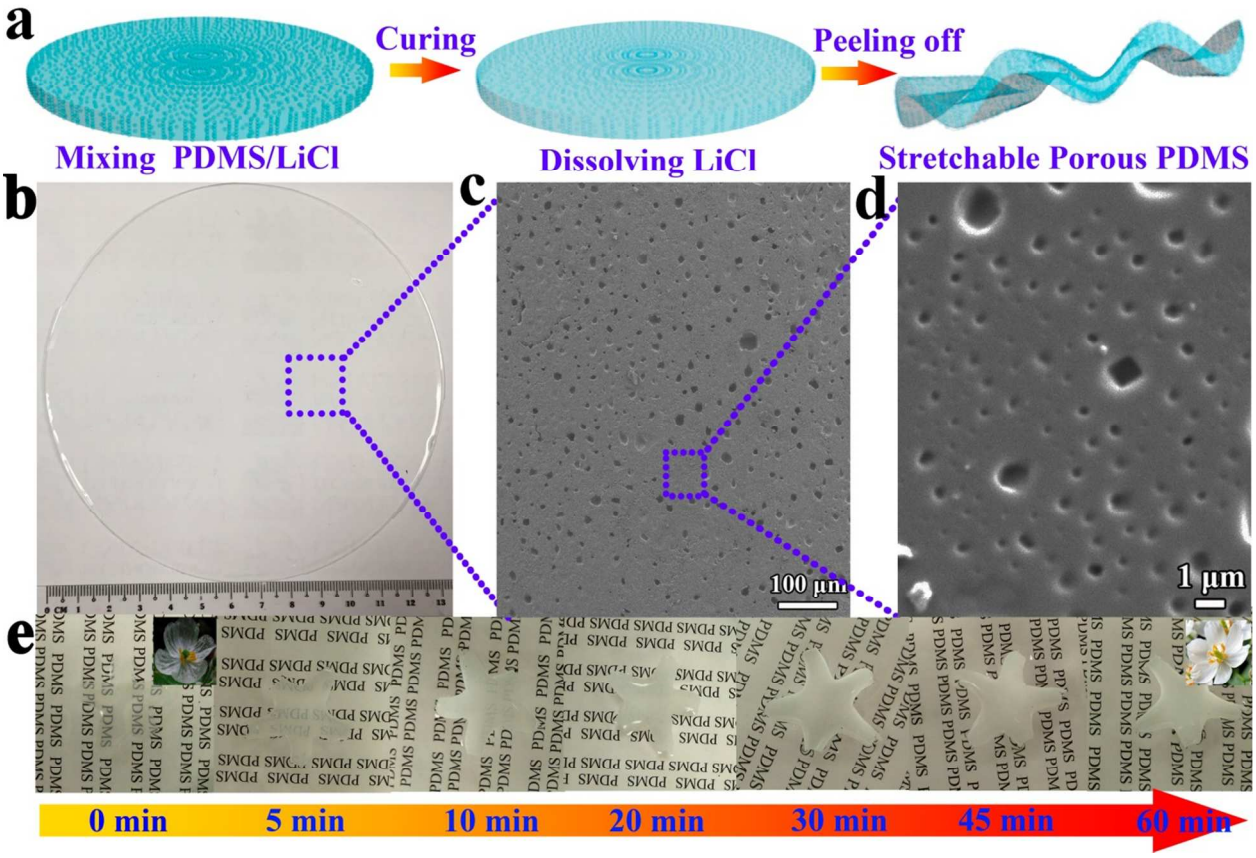

Figure 1 (a) Schematic illustration of fabrication procedure of the porous PDMS film. (b) Photo of the porous PDMS film with size of about 120 cm^2. (c,d) SEM images of the porous PDMS film. (e) The color changes of the porous PDMS after immersing in water for 60 min (insets are the photographs of *diphylleia grayi* at the wet state (left) and the dry state (right)).

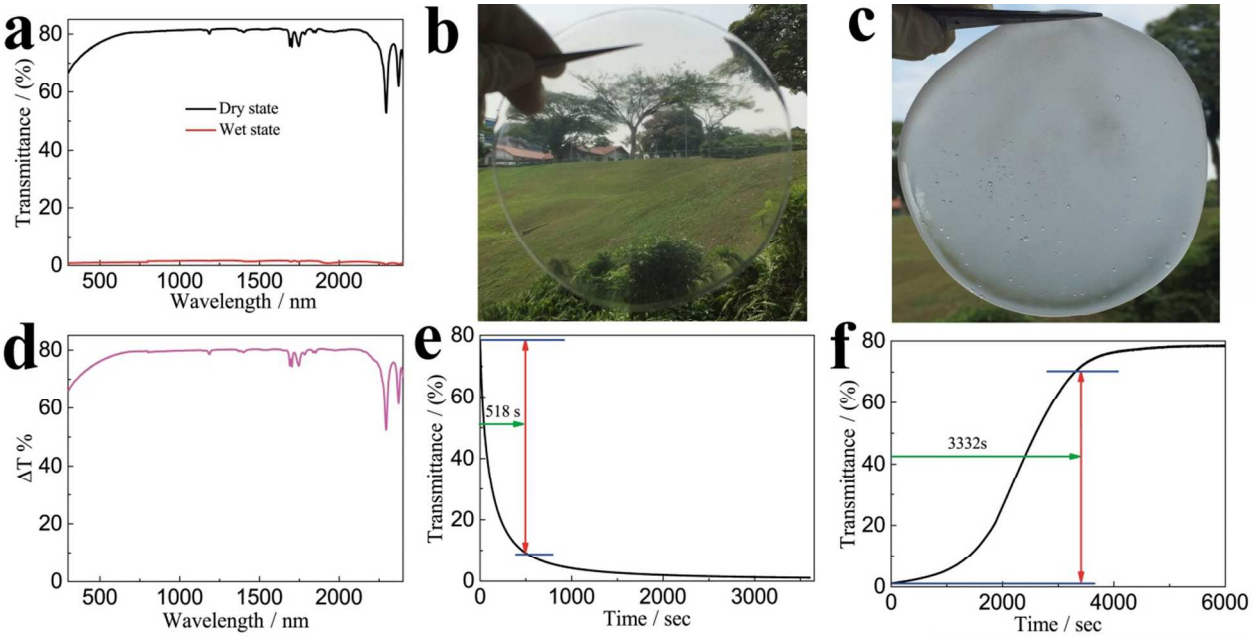

Figure 2 (a) The transmittance spectra of the porous PDMS with thickness of 0.4 mm and ratio of 5 wt% LiCl in the dry and wet states. Photographs of the porous PDMS with thickness of 0.4 mm in the (b) dry and (c) wet states, respectively. (d) Optical modulation of the porous PDMS with thickness of 0.4 mm. *In-situ* transmittance response of porous PDMS with thickness of 0.4 mm measured at 633 nm in the (e) coloring process (wetting process), and (f) bleaching process (drying process).

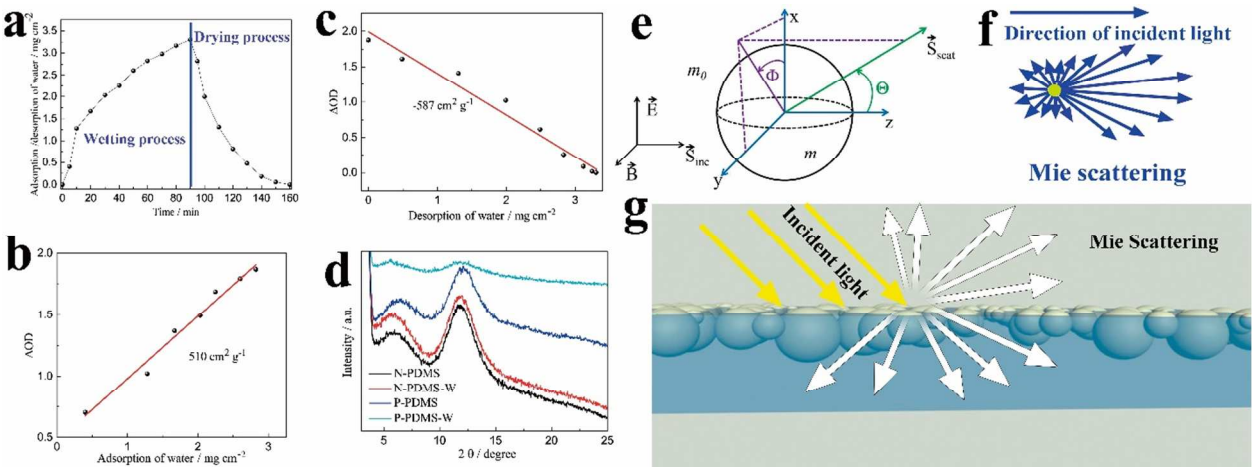

Figure 3 (a) The weight changes of the porous PDMS film after immersing it in water for 90 min, then take it out from the water and leave it in air for 70 min. (b) Optical density as a function of the adsorption water at 633 nm. (c) Optical density as a function of the desorption water at 633 nm. (d) XRD patterns of the normal PDMS and porous PDMS at the dry and wet states, respectively (N-PDMS, N-PDMS-W, P-PDMS, P-PDMS-W represent the normal PDMS at the dry state, the normal PDMS at the wet state, the porous PDMS at the dry state and the porous PDMS at the wet state, respectively). (e) Coordinate geometry for Mie scattering (m_o and m represent the refractive index of the surrounding medium and the scattering particle, respectively). (f) Schematic of Mie scattering. (g) A graphic about Mie scattering of the porous PDMS at the wet state.

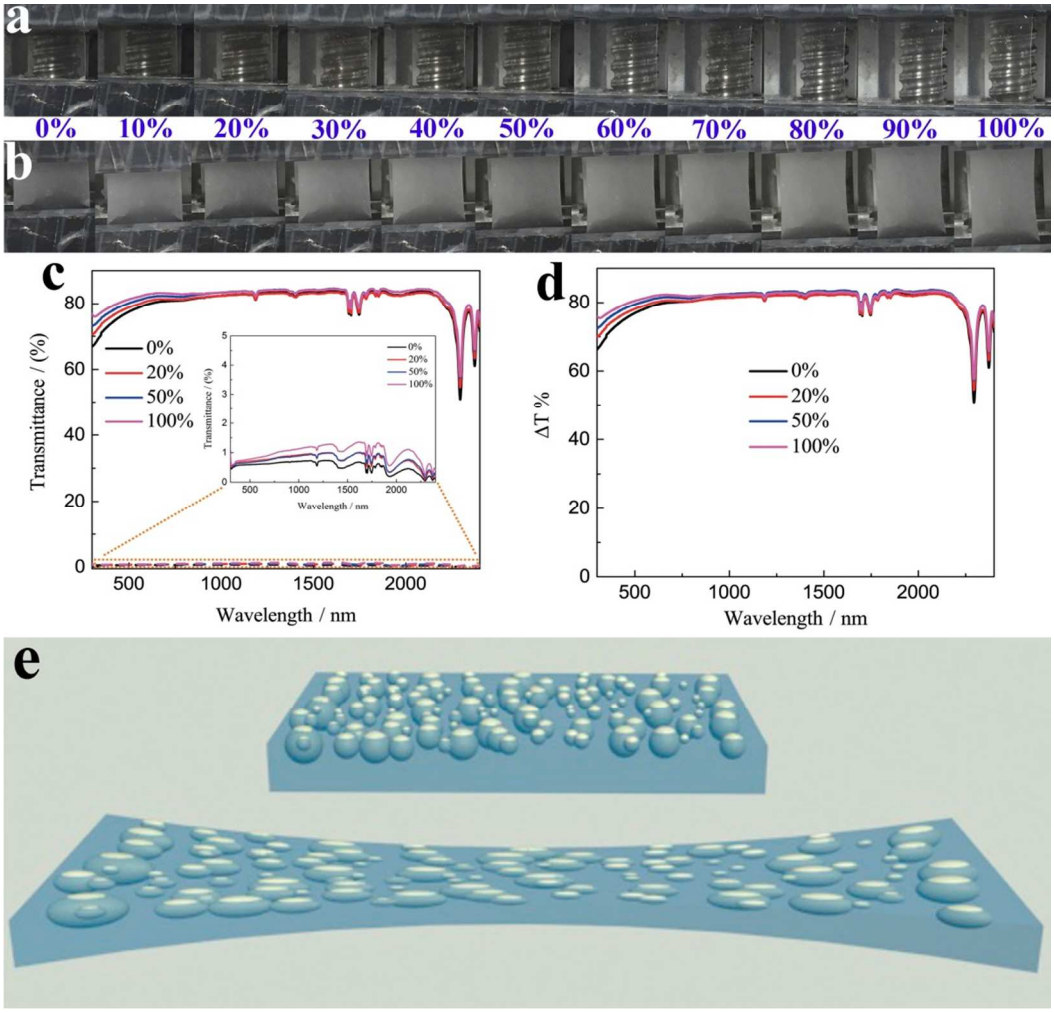

Figure 4 (a) Photographs of the porous PDMS film in the dry state stretched to different strains. (b) Photographs of the porous PDMS film in the wet state stretched to different strains. (c) The transmittance spectra of the porous PDMS stretched to different strains in the dry and wet states. (d) The optical modulation of the porous PDMS stretched to different strains in the dry and wet states. (e) The graphic of the wet porous PDMS under 0% strain (up) and 100% (bottom) strain states.

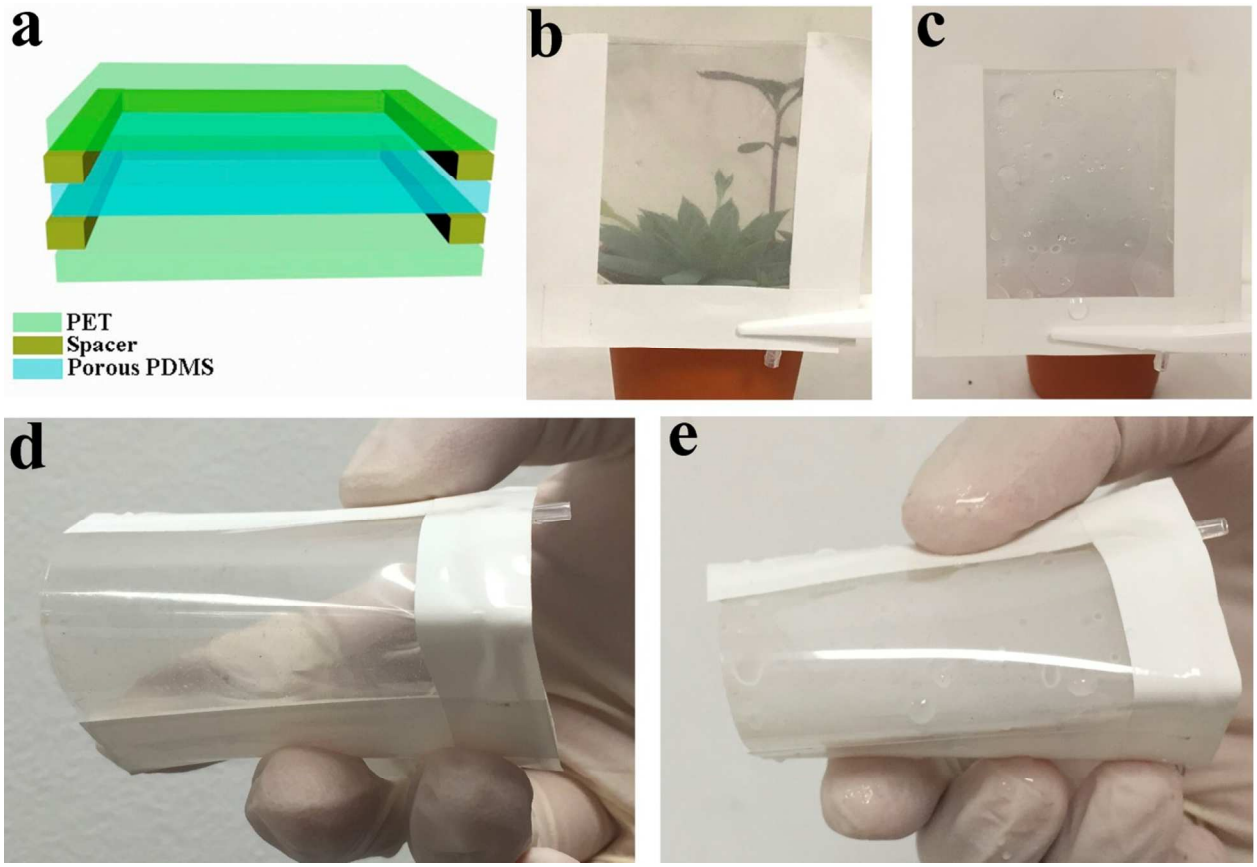

Figure 5 (a) The configuration of the smart window based on porous PDMS film. Photographs of the potted plants through the smart window in the (b) bleached state and (c) wet state. (d, e) Photographs of the smart window at bent state in both bleached and wet states, respectively.

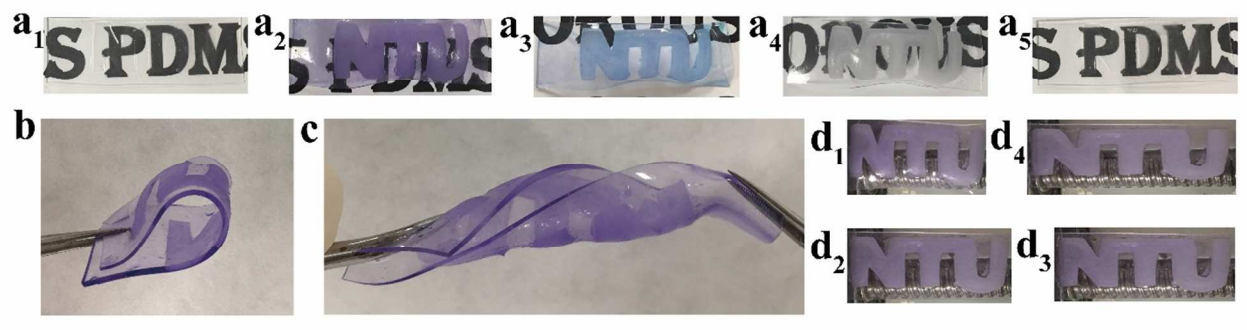

Figure 6 (a) Photographs of the porous PDMS film with pattern of NTU letters in different states; (a_1) in dry state (a_2) after immersing in toluidine blue O (0.5 wt%) aqueous solution for 12 h. (a_3) after immersing in ethanol for 1 s. (a_4) after immersing in water for 12 h. (a_5) after drying in air again. (b) Photographs of the porous PDMS film with pattern of NTU letters in bent state. (c) Photographs of the porous PDMS film with pattern of NTU letters in twist state. (d) Photographs of the porous PDMS film with pattern of NTU letters in different stretched states; (d_1) 0% strain state, (d_2) 20% strain state, (d_3) 30% strain state, (d_4) 50% strain state.

For Table of Contents Only